



Search for the $(1540)^+$ pentaquark using kaon secondary interactions at Belle

K. Abe,⁹ K. Abe,⁴⁷ I. Adachi,⁹ H. Aihara,⁴⁹ K. Aoki,²³ K. Arinstein,² Y. Asano,⁵⁴
T. Aso,⁵³ V. Aulchenko,² T. Aushev,¹³ T. Aziz,⁴⁵ S. Bahinipati,⁵ A. M. Bakich,⁴⁴
V. Balagura,¹³ Y. Ban,³⁶ S. Banerjee,⁴⁵ E. Barberio,²² M. Barbero,⁸ A. Bay,¹⁹ I. Bedny,²
U. Bitenc,¹⁴ I. Bizjak,¹⁴ S. Blyth,²⁵ A. Bondar,² A. Bozek,²⁹ M. Bracko,^{9,21,14}
J. Brodzicka,²⁹ T. E. Browder,⁸ M.-C. Chang,⁴⁸ P. Chang,²⁸ Y. Chao,²⁸ A. Chen,²⁵
K.-F. Chen,²⁸ W. T. Chen,²⁵ B. G. Cheon,⁴ C.-C. Chiang,²⁸ R. Chistov,¹³ S.-K. Choi,⁷
Y. Choi,⁴³ Y. K. Choi,⁴³ A. Chuvikov,³⁷ S. Cole,⁴⁴ J. Dalseno,²² M. Danilov,¹³ M. Dash,⁵⁶
L. Y. Dong,¹¹ R. Dowd,²² J. Dragic,⁹ A. Dnutskey,⁵ S. Edelmann,² Y. Enari,²³ D. Epifanov,²
F. Fang,⁸ S. Fratina,¹⁴ H. Fuji,⁹ N. Gabyshev,² A. Gamash,³⁷ T. Gershon,⁹ A. Go,²⁵
G. Gokhroo,⁴⁵ P. Goldenzweig,⁵ B. Golob,^{20,14} A. Gorisek,¹⁴ M. Grosse Perdekamp,³⁸
H. Guler,⁸ R. Guo,²⁶ J. Haba,⁹ K. Hara,⁹ T. Hara,³⁴ Y. Hasegawa,⁴² N. C. Hastings,⁴⁹
K. Hasuko,³⁸ K. Hayasaka,²³ H. Hayashii,²⁴ M. Hazumi,⁹ T. Higuchi,⁹ L. Hinze,¹⁹ T. Hojo,³⁴
T. Hokuue,²³ Y. Hoshi,⁴⁷ K. Hoshina,⁵² S. Hou,²⁵ W.-S. Hou,²⁸ Y. B. Hsiung,²⁸
Y. Igarashi,⁹ T. Iijima,²³ K. Ikado,²³ A. Imoto,²⁴ K. Inami,²³ A. Ishikawa,⁹ H. Ishino,⁵⁰
K. Itoh,⁴⁹ R. Itoh,⁹ M. Iwasaki,⁴⁹ Y. Iwasaki,⁹ C. Jacoby,¹⁹ C.-M. Jen,²⁸ R. Kagan,¹³
H. Kakuno,⁴⁹ J. H. Kang,⁵⁷ J. S. Kang,¹⁶ P. Kapusta,²⁹ S. U. Kataoka,²⁴ N. Katayama,⁹
H. Kawai,³ N. Kawamura,¹ T. Kawasaki,³¹ S. Kazi,⁵ N. Kent,⁸ H. R. Khan,⁵⁰
A. Kobayashi,⁵⁰ H. Kichimi,⁹ H. J. Kim,¹⁸ H. O. Kim,⁴³ J. H. Kim,⁴³ S. K. Kim,⁴¹
S. M. Kim,⁴³ T. H. Kim,⁵⁷ K. Kinoshita,⁵ N. Kishimoto,²³ S. Koirar,^{21,14} Y. Kozakai,²³
P. Krizan,^{20,14} P. Krokovny,⁹ T. Kubota,²³ R. Kulasiri,⁵ C. C. Kuo,²⁵ H. Kurashiro,⁵⁰
E. Kurihara,³ A. Kusaka,⁴⁹ A. Kuzmin,² Y.-J. Kwon,⁵⁷ J. S. Lange,⁶ G. Leder,¹²
S. E. Lee,⁴¹ Y.-J. Lee,²⁸ T. Lesiak,²⁹ J. Li,⁴⁰ A. Limosani,⁹ S.-W. Lin,²⁸ D. Liventsev,¹³
J. Madnaughton,¹² G. Majumder,⁴⁵ F. Mandl,¹² D. Marlow,³⁷ H. Matsumoto,³¹
T. Matsumoto,⁵¹ A. Matyjka,²⁹ Y. Miki,⁴⁸ W. Mitaro,¹² K. Miyabayashi,²⁴ H. Miyake,³⁴
H. Miyata,³¹ Y. Miyazaki,²³ R. Mizuk,¹³ D. Mohapatra,⁵⁶ G. R. Moliney,²² T. Mori,⁵⁰
A. Murakami,³⁹ T. Nagamine,⁴⁸ Y. Nagasaka,¹⁰ T. Nakagawa,⁵¹ I. Nakamura,⁹
E. Nakano,³³ M. Nakao,⁹ H. Nakazawa,⁹ Z. Natkaniec,²⁹ K. Neichi,⁴⁷ S. Nishida,⁹
O. Nito,⁵² S. Noguchi,²⁴ T. Nozaki,⁹ A. Ogawa,³⁸ S. Ogawa,⁴⁶ T. Ohshima,²³ T. Okabe,²³
S. Okuno,¹⁵ S. L. Olsen,⁸ Y. Onuki,³¹ W. Ostrowicz,²⁹ H. Ozaki,⁹ P. Pakhlov,¹³ H. Palka,²⁹
C. W. Park,⁴³ H. Park,¹⁸ K. S. Park,⁴³ N. Parslow,⁴⁴ L. S. Peak,⁴⁴ M. Pemicka,¹²
R. Pestotnik,¹⁴ M. Peters,⁸ L. E. Piihonen,⁵⁶ A. Poluektov,² F. J. Ronga,⁹ N. Root,²
M. Rozanska,²⁹ H. Sahoo,⁸ M. Saigo,⁴⁸ S. Saitoh,⁹ Y. Sakai,⁹ H. Sakamoto,¹⁷
H. Sakaue,³³ T. R. Sarangi,⁹ M. Satapathy,⁵⁵ N. Sato,²³ N. Satoyama,⁴² T. Schiester,¹⁹
O. Schneider,¹⁹ P. Schonmeyer,⁴⁸ J. Schumann,²⁸ C. Schwanda,¹² A. J. Schwartz,⁵
T. Seki,⁵¹ K. Senyo,²³ R. Seuster,⁸ M. E. Sevier,²² T. Shibata,³¹ H. Shibuya,⁴⁶
J.-G. Shiu,²⁸ B. Shwartz,² V. Sidorov,² J. B. Singh,³⁵ A. Somov,⁵ N. Soni,³⁵ R. Stamen,⁹
S. Stanic,³² M. Staric,¹⁴ A. Sugiyama,³⁹ K. Sumisawa,⁹ T. Sumiyoshi,⁵¹ S. Suzuki,³⁹

S. Y. Suzuki,⁹ O. Tajima,⁹ N. Takada,⁴² F. Takasaki,⁹ K. Tamai,⁹ N. Tamura,³¹
 K. Tanabe,⁴⁹ M. Tanaka,⁹ G. N. Taylor,²² Y. Teramoto,³³ X. C. Tian,³⁶ K. Trabelsi,⁸
 Y. F. Tse,²² T. Tsuboyama,⁹ T. T sukamoto,⁹ K. Uchida,⁸ Y. Uchida,⁹ S. Uehara,⁹
 T. Uglav,¹³ K. Ueno,²⁸ Y. Unno,⁹ S. Uno,⁹ P. Urquijo,²² Y. Ushiroda,⁹ G. Vamer,⁸
 K. E. Varvell,⁴⁴ S. Villa,¹⁹ C. C. Wang,²⁸ C. H. Wang,²⁷ M. -Z. Wang,²⁸ M. Watanabe,³¹
 Y. Watanabe,⁵⁰ L. Widham,¹² C. H. Wu,²⁸ Q. L. Xie,¹¹ B. D. Yabsley,⁵⁶ A. Yamaguchi,⁴⁸
 H. Yamamoto,⁴⁸ S. Yamamoto,⁵¹ Y. Yamashita,³⁰ M. Yamachi,⁹ Heyoung Yang,⁴¹
 J. Yang,³⁶ S. Yoshino,²³ Y. Yuan,¹¹ Y. Yusa,⁴⁸ H. Yuta,¹ S. L. Zang,¹¹ C. C. Zhang,¹¹
 J. Zhang,⁹ L. M. Zhang,⁴⁰ Z. P. Zhang,⁴⁰ V. Zhilich,² T. Ziegler,³⁷ and D. Zuercher¹⁹

(The Belle Collaboration)

¹Aomori University, Aomori

²Budker Institute of Nuclear Physics, Novosibirsk

³Chiba University, Chiba

⁴Chonnam National University, Kwangju

⁵University of Cincinnati, Cincinnati, Ohio 45221

⁶University of Frankfurt, Frankfurt

⁷Gyeongsang National University, Chinju

⁸University of Hawaii, Honolulu, Hawaii 96822

⁹High Energy Accelerator Research Organization (KEK), Tsukuba

¹⁰Hiroshima Institute of Technology, Hiroshima

¹¹Institute of High Energy Physics,

Chinese Academy of Sciences, Beijing

¹²Institute of High Energy Physics, Vienna

¹³Institute for Theoretical and Experimental Physics, Moscow

¹⁴J. Stefan Institute, Ljubljana

¹⁵Kanagawa University, Yokohama

¹⁶Korea University, Seoul

¹⁷Kyoto University, Kyoto

¹⁸Kyungpook National University, Taegu

¹⁹Swiss Federal Institute of Technology of Lausanne, EPFL, Lausanne

²⁰University of Ljubljana, Ljubljana

²¹University of Maribor, Maribor

²²University of Melbourne, Victoria

²³Nagoya University, Nagoya

²⁴Nara Women's University, Nara

²⁵National Central University, Chung-li

²⁶National Kaohsiung Normal University, Kaohsiung

²⁷National United University, Miao Li

²⁸Department of Physics, National Taiwan University, Taipei

²⁹H. Niewodniczanski Institute of Nuclear Physics, Krakow

³⁰Nippon Dental University, Niigata

³¹Niigata University, Niigata

³²Nova Gorica Polytechnic, Nova Gorica

³³O saka City University, O saka

³⁴O saka University, O saka

³⁵Panjab University, Chandigarh

- ³⁶Peking University, Beijing
- ³⁷Princeton University, Princeton, New Jersey 08544
- ³⁸RIKEN BNL Research Center, Upton, New York 11973
- ³⁹Saga University, Saga
- ⁴⁰University of Science and Technology of China, Hefei
- ⁴¹Seoul National University, Seoul
- ⁴²Shinshu University, Nagano
- ⁴³Sungkyunkwan University, Suwon
- ⁴⁴University of Sydney, Sydney NSW
- ⁴⁵Tata Institute of Fundamental Research, Bombay
- ⁴⁶Toho University, Funabashi
- ⁴⁷Tohoku Gakuin University, Tagajō
- ⁴⁸Tohoku University, Sendai
- ⁴⁹Department of Physics, University of Tokyo, Tokyo
- ⁵⁰Tokyo Institute of Technology, Tokyo
- ⁵¹Tokyo Metropolitan University, Tokyo
- ⁵²Tokyo University of Agriculture and Technology, Tokyo
- ⁵³Toyama National College of Maritime Technology, Toyama
- ⁵⁴University of Tsukuba, Tsukuba
- ⁵⁵Utkal University, Bhubaneswar
- ⁵⁶Virginia Polytechnic Institute and State University, Blacksburg, Virginia 24061
- ⁵⁷Yonsei University, Seoul

Abstract

Using kaon secondary interactions in the material of the Belle detector, we search for both inclusive and exclusive production of the $(1540)^+$. We set an upper limit of 2.5% at the 90% C.L. on the ratio of the $(1540)^+$ to (1520) inclusive production cross sections. We also search for the $(1540)^+$ as an intermediate resonance in the charge exchange reaction $K^+ n \rightarrow p K_S^0$. An upper limit of $\Gamma < 0.64 \text{ MeV}$ at the 90% C.L. at $m_{\text{res}} = 1.539 \text{ MeV} = c^2$ is set. These results are obtained from a 397 fb^{-1} data sample collected with the Belle detector near the $(4S)$ resonance, at the KEKB asymmetric energy e^+e^- collider.

PACS numbers: 13.75.Jz, 14.20.Jn, 14.80.-j

I. INTRODUCTION

The observation of the $(1540)^+$ pentaquark is one of the biggest mysteries of recent years (see [1] for the experimental overview). The $(1540)^+$ was first observed in exclusive reactions at low energy [1]. Later several groups reported observation in inclusive reactions at higher energies [1]. Conversely, other experiments at high energies do not see the $(1540)^+$ pentaquark although they do observe significantly larger yields of conventional hyperons than seen at the experiments that observe the $(1540)^+$. In order to resolve this discrepancy it is frequently assumed that pentaquark production decreases rapidly with energy. A high statistics experiment at low energies is therefore important. In order to achieve this, Belle utilises the small fraction of tracks that interact with the material of the inner part of the detector. These secondary interactions are used to search for pentaquarks. Particles produced in e^+e^- annihilation at Belle have quite low momenta; the most probable kaon momentum is only $0.6 \text{ GeV} = c$.

Results from two analyses are presented. In the first, we search for inclusive production of the $(1540)^+$ via the $K N \rightarrow (1540)^+ X$, $(1540)^+ \rightarrow p K_S^0$ process, using the signal from inclusive (1520) production as a reference. In the second, we search for exclusive $(1540)^+$ production in the charge exchange reaction $K^+ n \rightarrow (1540)^+ \rightarrow p K_S^0$. For this search, the yield of charge exchange reactions is used as a reference, allowing a direct comparison to the results of the DIANA experiment [2].

II. DETECTOR AND DATA SET

These studies are performed using a 357 fb^{-1} data sample collected at the $(4S)$ resonance and 40 fb^{-1} at an energy 60 MeV below the resonance. The data were collected with the Belle detector [3] at the KEKB asymmetric energy e^+e^- storage rings [4].

The Belle detector is a large-solid-angle magnetic spectrometer that consists of a silicon vertex detector (SVD), a 50-layer cylindrical drift chamber (CDC), an array of aerogel threshold Cherenkov counters (ACC), a barrel-like array of time-of-flight scintillation counters (TOF), and an array of CsI(Tl) crystals (ECL) located inside a superconducting solenoidal coil that produces a 1.5 T magnetic field. An iron flux return located outside the coil is instrumented to detect muons and K_L mesons (KLM). Two different inner detector configurations were used. For the first sample of 155 fb^{-1} , a 2.0 cm radius beam pipe and a 3-layer silicon vertex detector (SVD1) were used; for the second sample of 242 fb^{-1} , a 1.5 cm radius beam pipe, and a four-layer silicon vertex detector (SVD2), and a small-cell inner drift chamber were used [5].

A GEANT [6] based Monte-Carlo (MC) simulation is used to model the production of secondary pK pairs, and to determine the detector resolution and acceptance.

III. SELECTION OF SECONDARY pK PAIRS

The analyses are performed by identifying pK^- , pK^+ and pK_S^0 produced at secondary vertices. Charged particle candidates are required to be positively identified based on the CDC ($dE = dx$), TOF and ACC information. In addition, proton and charged kaon candidates are removed if they are consistent with being electrons based on ECL, CDC and ACC information. K_S^0 candidates are reconstructed from p^- pairs that have masses within

10 MeV $=c^2$ of the nominal K_S^0 mass (3 σ window). Additional selection requirements are imposed on the quality of the K_S^0 vertex, on the impact parameters of the daughter tracks and on the angle between the momentum and the direction from the interaction point (IP) to the vertex.

The proton and kaon candidates are required to have an origin that is displaced from the IP. The pK^- , pK^+ and pK_S^0 vertices are fitted and those with a radial distance $1 < R < 11$ cm are selected. Additional criteria on the quality of the pK vertex are applied. We consider secondary pK pairs only in the central part of the detector $0.74 < \cos \theta < 0.9$, where θ is the polar angle of the secondary pK vertex. The distributions of the secondary pK_S^0 vertices in the xy plane are shown in Fig. 1 for the SVD 1 and SVD 2 data samples, where the z -axis passes through the IP and is antiparallel to the e^+ beam. The beam pipe,

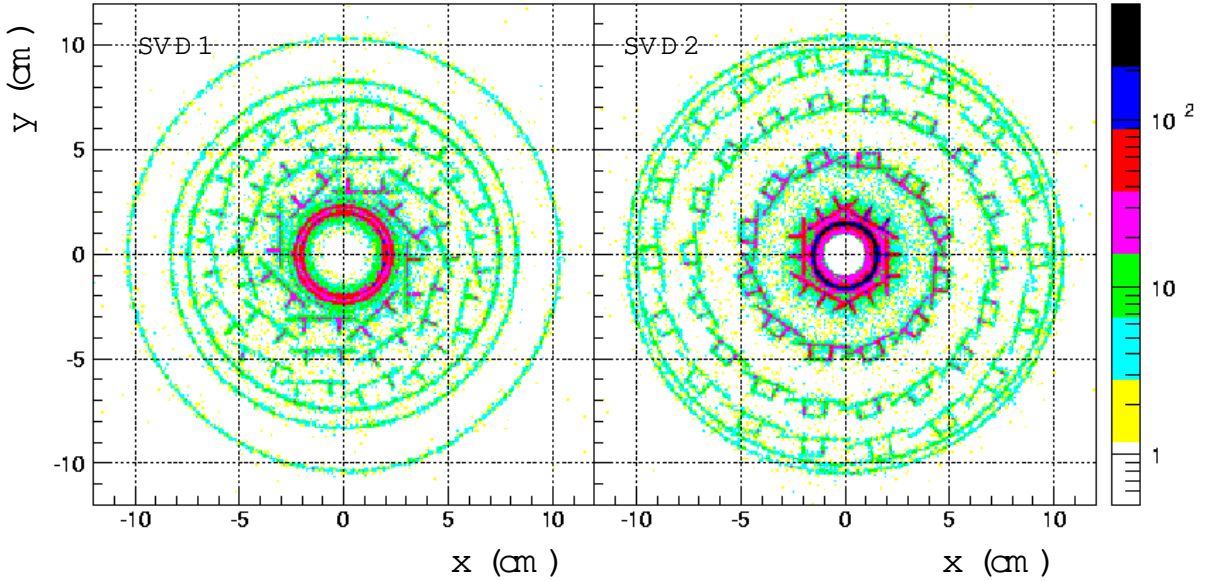


FIG. 1: Distribution of reconstructed secondary pK_S^0 vertices in the Belle detector for the SVD 1 (left) and SVD 2 (right) data samples.

the SVD layers, the SVD cover and the CDC support cylinders are clearly visible.

IV. SEARCH FOR INCLUSIVE $(1540)^+$ PRODUCTION

The mass spectra for pK^- and pK_S^0 secondary vertices are shown in Fig. 2. We apply an additional selection requirement on the angle between the pK momentum and the direction from the IP to the pK vertex $d < 1$ rad. In the pK^- sample we reject $! p$ and $K_S^0 !$ $^+$ decays misidentified as secondary pK^- vertices. No significant structures are observed in the $m_{pK_S^0}$ spectrum, while in the m_{pK^-} spectrum a (1520) signal is clearly visible. The pK^- mass spectrum is fitted to a sum of a (1520) signal function and a threshold function. The signal function is a D-wave Breit-Wigner shape convolved with a detector resolution function, determined from MC. The detector resolution function is parametrized by a double Gaussian with widths of 2 MeV and 5 MeV with approximately equal contributions from each Gaussian component. The (1520) parameters obtained from the fit are consistent with the

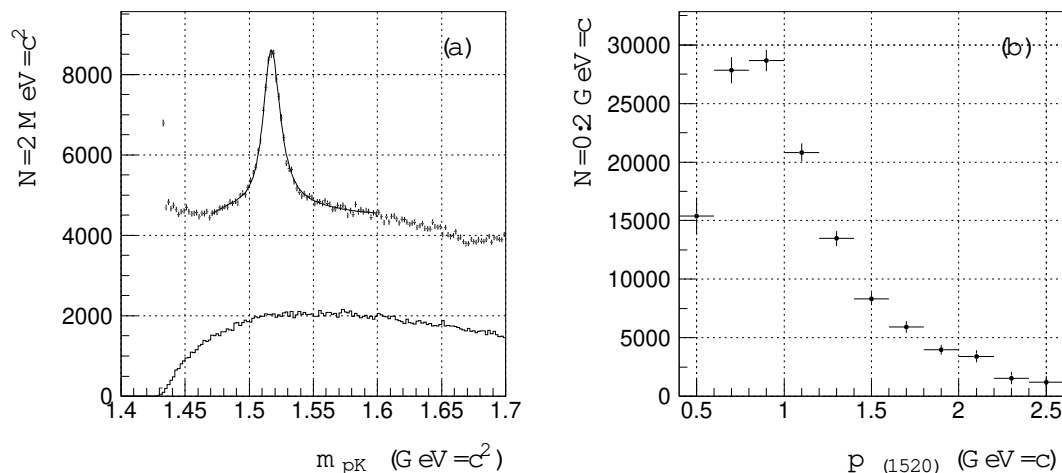


FIG. 2: (a) Mass spectra of pK (points with error bars) and pK_s^0 (histogram) secondary pairs. The fit is described in the text. (b) Momentum spectrum of the (1520) .

PDG values [7]. The (1520) yield, defined as the fit function signal component integrated over the $1.48\{1.56\text{ GeV} = c^2$ mass interval (2.5%), is $(4.02 \pm 0.08) \cdot 10^6$ events.

The pK_s^0 mass spectrum is fitted to a sum of a $(1540)^+$ signal component and a third order polynomial. The $(1540)^+$ is assumed to be narrow and its shape is determined by the detector resolution function, which is again a double Gaussian with similar parameters to those of used for the pK mode. The MC resolution is checked against data using the $\Lambda^0 K^+$ signal, which has a topology similar to the secondary pK_s^0 pairs. It is found that the width is 4% percent larger in data than in MC, and this correction factor is applied to the mass resolution of secondary pK_s^0 vertices. For $m = 1540\text{ MeV} = c^2$ the fit yield is 58 ± 129 events. Using the Feldman-Cousins method of upper limit evaluation [8], we find $N < 270$ events at the 90% C.L. The upper limit is below 320 events for a wide range of possible $(1540)^+$ masses. We set an upper limit on the ratio of $(1540)^+$ to (1520) production cross sections:

$$\frac{N_{(1540)^+} \cdot B(pK)}{N_{(1520)} \cdot B(pK_s^0)} \frac{B((1520) \rightarrow pK)}{B((1540)^+ \rightarrow pK_s^0) \cdot B(K_s^0 \rightarrow \Lambda^0 K^+)} < 2.5\% \text{ at the } 90\% \text{ C.L.}$$

It is assumed that $B((1540)^+ \rightarrow pK_s^0) = 25\%$. We take $B((1520) \rightarrow pK) = \frac{1}{2} B((1520) \rightarrow N K) = \frac{1}{2}(45 \pm 1)\%$ [7]. The ratio of efficiencies for $(1540)^+ \rightarrow pK_s^0$ and $(1520) \rightarrow pK$ is obtained from MC simulation assuming that the two processes have similar kinematics. Our limit is much lower than the results reported by many experiments that observe the $(1540)^+$. For example it is two orders of magnitude lower than the value reported by the HERMES Collaboration [9].

The momentum spectrum of the produced (1520) is shown in Fig. 2 (b). This spectrum is obtained by fitting m_{pK} in momentum bins and correcting for the efficiency obtained from the MC. If a (1520) is produced as an intermediate resonance in the elastic scattering of a K^- on a free proton, then its momentum is around $400\text{ MeV} = c$. As such, the observed hard momentum spectrum of the (1520) confirms that they are produced in inelastic interactions. We find that non-strange particles do not produce (1520) since the secondary pK pairs are accompanied by an additional K^+ from the same vertex in only about 0.5% of events.

The projectiles that can produce (1520) are K^+ , K_S^0 , K_L and π^+ . The π^+ needs a momentum of about $1.8 \text{ GeV}/c$ to produce the (1520). The number of such π^+ 's in e^+e^- annihilations is small. The observed number of (1520) can not be produced by π^+ projectiles even if the total N cross section is assumed to be saturated by inclusive (1520) production. We therefore conclude that our (1520) signal is due to kaon interactions, with a contribution of π^+ interactions no larger than a few percent.

V. SEARCH FOR EXCLUSIVE $(1540)^+$ PRODUCTION

Possible exclusive pentaquark production is studied using the $K^+n \rightarrow pK_S^0$ reaction, searching for the $(1540)^+$ as an intermediate resonance. Since the projectile is not reconstructed, it is not possible to distinguish this reaction from the reactions $K_S^0p \rightarrow pK_S^0$, $K_L^0p \rightarrow pK_S^0$, and inelastic reactions with a π^0 or undetected tracks in the final state. Therefore we apply selection criteria which suppress the contribution of the inelastic reactions in the sample of secondary pK_S^0 pairs (see section V E), and determine the contribution of the charge exchange reaction indirectly, as described below in this section. The cross section of the $K_S^0p \rightarrow (1540)^+ \rightarrow pK_S^0$ reaction is expected to be similar to the cross section of the $K^+n \rightarrow (1540)^+ \rightarrow pK_S^0$ reaction [10], however the flux of K_S^0 is decreased by decays in flight and we conservatively neglect the contribution of this reaction. The $K_L^0p \rightarrow pK_S^0$ reaction can produce a dip in the $(1540)^+$ region because of the interference of resonant and nonresonant amplitudes. However, the size of the dip is expected to be negligible [10].

The number of charge exchange reactions can be estimated in a straightforward way using the known flux of primary K^+ , K^+ , the reaction cross section, σ^{ch} , the amount of material, M , and the reconstruction efficiency for the secondary pK_S^0 pair, $\epsilon_{pK_S^0}$, and taking into account nuclear effects:

$$N^{ch}(m_{pK}) = \int^Z K^+ \sigma^{ch} M_{pK_S^0} B S(E_N; \mathbf{p}_F) \left(\frac{p}{s} - m_{pK} \right) P dE_N d^3p_F dp_{K^+} dR d\Omega; \quad (1)$$

where B is the product of K^0 branching fractions $B = B(K^0 \rightarrow K_S^0) B(K_S^0 \rightarrow p^+)$, $S(E_N; \mathbf{p}_F)$ is a nuclear spectral function which is a joint probability to find in a nucleus a nucleon with energy E_N and Fermi momentum \mathbf{p}_F , $s = (E_{K^+} + E_N)^2 - (\mathbf{p}_{K^+} + \mathbf{p}_F)^2$ is the centre of mass (c.m.) energy of the reaction squared, E_{K^+} is the energy and \mathbf{p}_{K^+} is the momentum of the projectile, m_{pK} is the mass of the produced pair, P is the probability that the produced pair is not rescattered in the nucleus and R and Ω are the radial distance and polar angle of the secondary vertex, respectively.

However, it is difficult to keep the systematic errors in this calculation under control, because M and $\epsilon_{pK_S^0}$ are complicated functions of the coordinates and the estimation of S and P is model dependent. This problem is solved by reconstructing the decay chain $D^0 \rightarrow \bar{D}^0$, $\bar{D}^0 \rightarrow K^+$ for events where a K^+ interacts elastically in the detector material. The reconstruction procedure is explained in detail in section V A. The yield of such decays, N_D^{el} , is expressed as

$$N_D^{el}(m_{pK}) = \int^Z K^+ \sigma^{el} M_{pK^+} S(E_N; \mathbf{p}_F) \left(\frac{p}{s} - m_{pK} \right) P dE_N d^3p_F dp_{K^+} dR d\Omega; \quad (2)$$

where K^+ is the flux of K^+ originating from the selected D^0 decay, σ^{el} is the cross section for elastic $K^+p \rightarrow pK^+$ scattering and ϵ_{pK^+} is the efficiency of reconstructing the

secondary pK^+ vertex. The nuclear suppression P is assumed to be the same for pK^+ pairs and pK^0 pairs produced in the charge exchange reaction. We express N^{ch} in terms of N_D^{el} . The expressions are simplified by the facts that the products $M_{pK_S^0}$ and M_{pK^+} are approximately independent of \mathbf{p}_{pK} for the central part of the detector; the ratio $M_{pK_S^0} = M_{pK^+}$ is approximately independent of the secondary pair momentum, \mathbf{p}_{pK} ; and the nuclear suppression P is approximately independent of \mathbf{p}_{pK} (see section V A). We approximate the nuclear spectral function as $S(E_N; \mathbf{p}_F) = W(\mathbf{p}_F) f(E_N - f(\mathbf{p}_F))$, where the function $f(\mathbf{p}_F)$ is defined so that $E_N = f(\mathbf{p}_F)$ corresponds to the maximum of $S(E_N; \mathbf{p}_F)$. We obtain

$$N^{\text{ch}}(m_{pK}) = N_D^{\text{el}}(m_{pK}) \frac{K^+(m_{pK})}{K_D^+(m_{pK})} \frac{\text{ch}(m_{pK})}{\text{el}(m_{pK})} \frac{pK_S^0(m_{pK})}{pK^+(m_{pK})} B; \quad (3)$$

where

$$\frac{K^+(m_{pK})}{K_D^+(m_{pK})} = \frac{R}{R} \frac{K^+(\mathbf{p}_{K^+}) W(\mathbf{p}_F)}{K^+(\mathbf{p}_{K^+}) W(\mathbf{p}_F)} \frac{\int_{\bar{s} - m_{pK}}^{\bar{s} - m_{pK}} p_{K^+}(m_{pK}; \mathbf{p}_{pK}) d^3p_F dp_{K^+}}{\int_{\bar{s} - m_{pK}}^{\bar{s} - m_{pK}} p_{K^+}(m_{pK}; \mathbf{p}_{pK}) d^3p_F dp_{K^+}}; \quad (4)$$

The p.d.f. of the Fermi momentum distribution $W(\mathbf{p}_F)$ is determined from data in section V A. The form of the $f(\mathbf{p}_F)$ is discussed in the same section. The integrations are described in section V B. Equation (3) provides the basic formula to determine the yield of the charge exchange reaction in our data sample. The formula (3) would be even simpler if we could use K^+ projectiles from D decays that undergo charge exchange in the detector material. However, the fraction of such events is very low because of the relatively small cross section, and the low K_S^0 reconstruction efficiency and branching fraction.

A. Determination of N_D^{el}

To determine the number of $D \rightarrow \bar{D}^0, \bar{D}^0 \rightarrow K^+$ decays for which a K^+ interacts elastically in the detector material, the four-momentum of the interacting K^+ is reconstructed based on the information available from the produced secondary pK^+ pair.

If a secondary pK pair is produced in a quasi-elastic reaction, four-momentum conservation implies

$$E_K + E_N = E_{pK}; \quad (5)$$

$$\mathbf{p}_K + \mathbf{p}_F = \mathbf{p}_{pK}; \quad (6)$$

The nucleon energy, E_N is approximated by [11]

$$E_N = m_N + \sqrt{2 \frac{\mathbf{p}_F^2}{2m_N}}; \quad (7)$$

where m_N is the nucleon mass and $\sqrt{2} M$ eV is the nucleon binding energy. This approximation is valid for the high \mathbf{p}_F part of the nuclear spectral function. Another possible approximation is $E_N = m_N + E_R$, where $E_R \approx 26$ M eV is the average removal energy of the bound nucleon. We find that both approximations give a similar resolution in the D^0 mass (see below) and our result is independent of the choice. The quantities E_{pK} and \mathbf{p}_{pK} are measured; taking into account the primary and secondary vertex constraints, Eqs (5)-(7) can then be solved iteratively.

The iterative process is started from Eq. (7) where some average value of \mathbf{p}_F is substituted. Then the energy of the projectile E_K is determined from Eq. (5). In the next step the projectile momentum \mathbf{p}_K is determined from its absolute value $p_K = \sqrt{E_K^2 - m_K^2}$, and the light direction obtained from the primary and secondary vertex constraints, taking into account the bending of the track in the magnetic field. The value of \mathbf{p}_F is then determined from Eq. (6) and the iteration loop is closed by substituting the obtained \mathbf{p}_F into Eq. (7).

The projectile four-momentum is determined for all secondary pK^+ pairs. The resulting K^+ projectile candidates are then combined with all the candidates in the event to form \bar{D}^0 candidates; the \bar{D}^0 candidates are combined with all the remaining candidates to form D^0 candidates. The candidates are required to be positively identified based on the CDC ($dE=dx$), TOF and ACC information and to originate from the vicinity of the IP. We reject vertices with additional tracks and require $50 < \mathbf{p}_F \cdot \mathbf{j} < 300 \text{ M eV} = c$. The lower bound on $\mathbf{p}_F \cdot \mathbf{j}$ is used to reject interactions on hydrogen (see below). Events in a $2 \text{ M eV} = c^2$ (3σ) window in $m_{D^0} = m_{D^0} + m_{\bar{D}^0}$ are selected and the mass of the daughter \bar{D}^0 candidates is plotted (see Fig. 3 (a)). A signal of $470 \pm 26 \bar{D}^0$ events with the mass consistent with the PDG

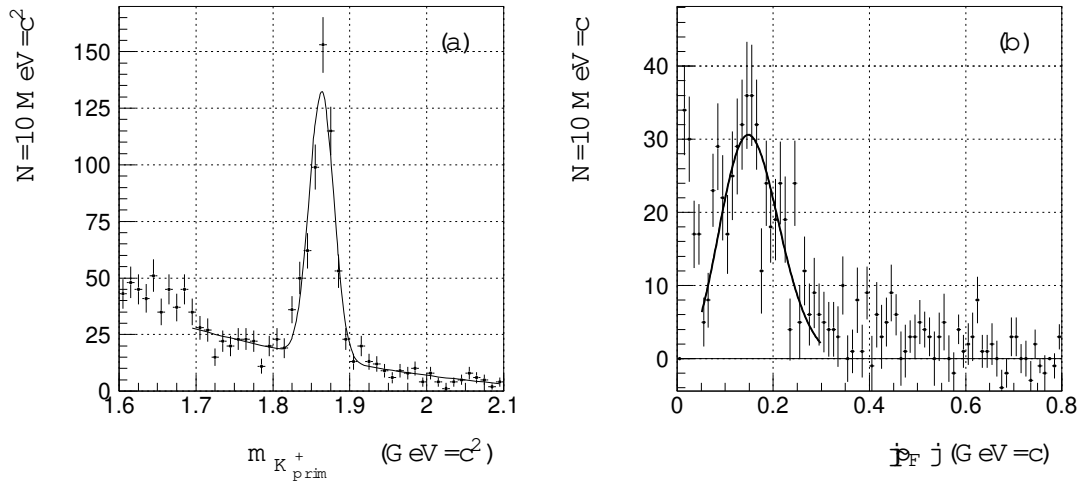


FIG. 3: (a) Invariant mass of the selected \bar{D}^0 candidates with the K^+ reconstructed via a secondary pK^+ vertex. (b) Sideband subtracted distribution of $\mathbf{p}_F \cdot \mathbf{j}$ for the selected \bar{D}^0 candidates, fitted to the oscillator model expectations.

value and a mass resolution of $16 \text{ M eV} = c^2$ is observed. The \bar{D}^0 signal and sideband regions are selected as $\mathbf{j} \cdot \mathbf{n}_{K^+} + m_{\bar{D}^0} \cdot \mathbf{j} < 50 \text{ M eV} = c^2$ and $60 < \mathbf{j} \cdot \mathbf{n}_{K^+} + m_{\bar{D}^0} \cdot \mathbf{j} < 110 \text{ M eV} = c^2$, respectively. The sideband subtracted distribution of $\mathbf{p}_F \cdot \mathbf{j}$ is shown in Fig. 3 (b). The peak near zero is attributed to interactions on hydrogen, which is present in the detector material. If $E_N = m_N$ is used instead of Eq. (7), this peak is found at zero, as expected for interactions with a free proton. The $\mathbf{p}_F \cdot \mathbf{j}$ spectrum is fitted to the parametrization, expected in the oscillator model [12]: $\mathbf{p}_F \cdot \mathbf{j} \left[1 + 4 = 3 (\mathbf{p}_F \cdot \mathbf{j} - p_0)^2 \right] \exp(-\mathbf{p}_F \cdot \mathbf{j}^2 - p_0^2)$. The value for the model parameter returned by the fit, $p_0 = 115 \pm 4 \text{ M eV} = c$, is in agreement with other measurements of the $\mathbf{p}_F \cdot \mathbf{j}$ distributions [12].

We find that the fraction of D^0 events in hydrogen peak is roughly independent on pair momentum. Since this fraction is inversely proportional to P (there can be no rescattering in hydrogen), we conclude, that P is also roughly independent on pair momentum, which is important to perform the integration in Eq. (4).

The m_{D^0} spectra are fitted in m_{pK} bins to determine the D^0 yield. The fit function is comprised of the sum of a Gaussian and a first order polynomial. The Gaussian mean and width, and the polynomial parameters, are all floated in the fit. The number of D^0 mesons in the $(1540)^+$ region is 24 ± 7 per $50 \text{ MeV} = c^2$ bin.

B. Determination of $K^+ = \frac{K^+}{D^0}$

The fluxes of primary K^+ 's and K^0 's from D^0 are determined from data. Primary K^+ candidates are required to originate from the vicinity of the IP and to be positively identified based on the CDC ($dE = dx$), TOF and ACC information. D^0 candidates are selected by combining the kaon candidate with pion candidates, in the same way as described above. Correction for reconstruction efficiency and contamination from other particle species is performed using MC that is calibrated from data. The integration in Eq. 4 is performed using a Monte Carlo technique. The nucleon Fermi momentum p_F is assumed to be isotropic relative to the projectile momentum p_K . The fact that the secondary pK pair efficiency depends on the momentum results in a correction of about 3% in the ratio. The flux ratio at $m_{pK} = 1539 \text{ GeV} = c^2$ is equal to 850 ± 20 ; the uncertainty is dominated by the assumption concerning the relation between E_N and $|p_F|$. For this measurement we use about 20% of the data sample distributed uniformly over the running period.

C. Determination of $\frac{ch}{el}$

The cross sections $\frac{ch}{el}$ and $\frac{el}{ch}$ are obtained from published data [7, 13]. The data are fitted with polynomials in m_{pK} , and the ratio of the fitted functions is used to obtain $\frac{ch}{el}$. The value of the ratio is 0.35 ± 0.02 at $m_{pK} = 1539 \text{ GeV} = c^2$ and rises with m_{pK} . Errors are assigned based on the typical experimental errors in the region of interest.

D. Determination of $\frac{pK_S^0}{pK^+}$

Monte Carlo simulations are used to estimate the ratio $\frac{pK_S^0}{pK^+}$. The angular distribution in the reaction c.m. frame is assumed to be uniform, as expected for low energy elastic K^+p scattering and for $(1540)^+ \rightarrow pK_S^0$ decay. We consider the following sources of systematic uncertainty: K_S^0, K^+ and secondary pK reconstruction efficiency (7%), uncertainty in material description (5%), uncertainty in the description of the reaction kinematics (5%), and the MC statistical uncertainty (5%). The ratio of efficiencies at $m_{pK} = 1539 \text{ GeV} = c^2$ is $(43 \pm 5)\%$. Here all the uncertainties are added in quadrature.

E. Upper limit on $(1540)^+$ yield in exclusive reaction

To suppress the contribution of inelastic reactions in the sample of secondary pK_S^0 pairs we reject vertices with additional tracks and require $50 < |p_F| < 300 \text{ MeV} = c$. The lower bound on $|p_F|$ is used to reject interactions on hydrogen, which do not contribute to the charge exchange reaction. The effect of angular cuts used by DIANA to suppress rescattering is checked, and found not to suppress background significantly when the $|p_F|$ cut is applied, and not to improve the sensitivity. The pK_S^0 mass spectrum and the expected yield from the

charge exchange reaction is shown in Fig. 4 (a). The statistical and systematic uncertainties

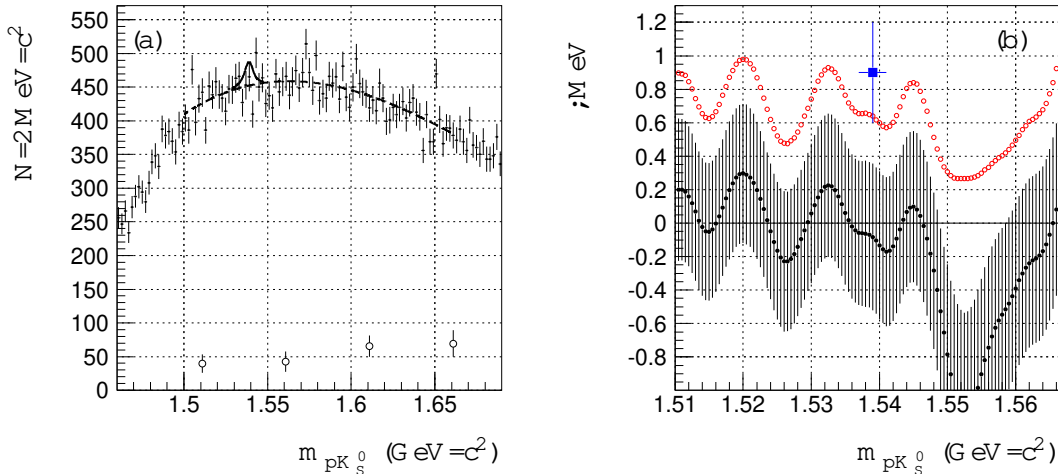


FIG. 4: (a) Invariant mass spectrum for secondary pK_S^0 pairs (small dots with error bars) and expected yield of the charge exchange reaction per $2M eV = c^2$ (open dots). A fit to a third order polynomial is shown with a dashed curve. The $(1540)^+$ contribution expected from the DIANA result is shown with solid line. (b) The yield of $(1540)^+$ from the fit, expressed in terms of the resonance width. The open dots correspond to the upper limit at the 90% C.L., obtained using the Feldman-Cousins method. The square with error bars indicates the current PDG value for the $(1540)^+$ width.

on N^{ch} are added in quadrature. In the $(1540)^+$ region we expect 206 ± 72 charge exchange events per $10M eV = c^2$ bin. The $m_{pK_S^0}$ distribution is fitted to a third order polynomial and a signal p.d.f. positioned at various values of $m_{pK_S^0}$. The fit yields $N_{+} = 11 \pm 59$ candidates at $m_{pK} = 1.539 GeV = c^2$. The ratio of the $(1540)^+$ yield to the charge exchange reaction yield can be expressed in terms of the $(1540)^+$ width (see for example [14]):

$$R_{+} = \frac{N_{+}}{N^{ch}} \frac{\Gamma^{ch}}{107 m b B_i B_f} 10M eV ;$$

where B_i and B_f are $(1540)^+$ branching fractions into initial and final states. We assume $B_i = B_f = 0.5$. The resulting values of R_{+} are shown as a function of m_{pK} in Fig. 4 (b). Also shown in Fig. 4 (b) are the 90% C.L. upper limits, obtained with the Feldman-Cousins method [8], and the current PDG value for the $(1540)^+$ width [7], which is based on the DIANA result. A similar width has been inferred from a reanalysis of K^+d scattering [15]. It is assumed that nuclear suppression for the $(1540)^+$ is the same as for nonresonant pK_S^0 pairs.

VI. CONCLUSIONS

Using kaon interactions in the material of the Belle detector, we searched for both inclusive and exclusive production of the $(1540)^+$. No $(1540)^+$ signal was found in the sample of

secondary pK_s^0 pairs. For inclusive production we set the following upper limit:

$$\frac{(K^+ n \rightarrow (1540)^+ X)}{(K^+ n \rightarrow (1520)X)} < 2.5\% \text{ at the } 90\% \text{ C.L.}$$

For exclusive production we find

$$(K^+ n \rightarrow (1540)^+ \rightarrow pK_s^0) < 0.64 M eV \text{ at the } 90\% \text{ C.L.}$$

at $m^+ = 1.539 M eV = c^2$. This upper limit is below the current PDG value of $= 0.9 - 0.3 M eV$, and below $1.0 M eV$ for a wide interval of possible $(1540)^+$ masses. This measurement uses a sample of low energy kaon interactions and allows for a direct comparison with the DIANA result. With similar sensitivity, our results do not support their evidence for the $(1540)^+$.

VII. ACKNOWLEDGEMENTS

We are grateful to A. Kaidalov and Yu. Kiselev for the fruitful discussions. We thank the KEKB group for the excellent operation of the accelerator, the KEK cryogenics group for the efficient operation of the solenoid, and the KEK computer group and the National Institute of Informatics for valuable computing and Super-SINET network support. We acknowledge support from the Ministry of Education, Culture, Sports, Science, and Technology of Japan and the Japan Society for the Promotion of Science; the Australian Research Council and the Australian Department of Education, Science and Training; the National Science Foundation of China under contract No. 10175071; the Department of Science and Technology of India; the BK21 program of the Ministry of Education of Korea and the CHEP SRC program of the Korea Science and Engineering Foundation; the Polish State Committee for Scientific Research under contract No. 2P03B 01324; the Ministry of Science and Technology of the Russian Federation; the Ministry of Higher Education, Science and Technology of the Republic of Slovenia; the Swiss National Science Foundation; the National Science Council and the Ministry of Education of Taiwan; and the U.S. Department of Energy.

-
- [1] K. Hicks hep-ex/0504027. Submitted to Prog. Part. Nucl. Phys.
 - [2] V. Bam in et al. (DIANA Collaboration), Phys. Atom. Nucl. 66 (2003), p. 1715.
 - [3] A. Abashian et al. (Belle Collaboration), Nucl. Instr. Meth. A 479 (2002), p. 117.
 - [4] S. Kurokawa and E. Kikutani, Nucl. Instr. Meth. A 499 (2003), p. 1.
 - [5] Y. Ushiroda (Belle SVD2 Group), Nucl. Instr. Meth. A 511 (2003), p. 6.
 - [6] R. Brun et al., GEANT 3.21, CERN Report DD/EE/84-1 (1984).
 - [7] S. Eidelman et al. (Particle Data Group), Phys. Lett. B 592 (2004), p. 1.
 - [8] G. J. Feldman and R. D. Cousins, Phys. Rev. D 57 (1998), p. 3873.
 - [9] A. Arapetian et al. (HERMES Collaboration), Phys. Lett. B 585 (2004), p. 213.
 - [10] A. Kaidalov, private communication.
 - [11] A. Sibirtsev et al., Eur. Phys. J. A 23 (2005), p. 491.
 - [12] B. M. Abramov et al., JETP Lett. 71 (2000), p. 359.

- [13] U. Casadei et al, CERN/HERA 75-1 (1975).
C.J.S. Damerell et al, Nucl. Phys. B 94 (1975), p. 374.
R.G. Gasser et al, Phys. Rev. D 15 (1977), p. 1200.
- [14] R.N. Cahn and G.H. Trilling, Phys. Rev. D 69 (2004), p. 11501.
- [15] W.R. Gibbs, Phys. Rev. C 70 (2004), p. 45208.